Advanced Mechanical and Mechatronic Systems

Research Article
Volume 2(1), 2026, 63–75
https://doi.org/10.53623/amms.v2i1.797

Gait Generation Using a Fourier Series for a Quadruped Robot with 2-DoF Legs

M. Munadi, Mochammad Ariyanto*

Department of Mechanical Engineering, Diponegoro University, Jl. Prof. Soedarto, Tembalang, Kec. Tembalang, Semarang 50275, Central Java, Indonesia

*Correspondence: mochammad_ariyanto@ft.undip.ac.id

SUBMITTED: 16 August 2025; REVISED: 16 November 2025; ACCEPTED: 19 November 2025

ABSTRACT: This study proposed the development of a quadruped cat robot designed to achieve straight-line walking motion inspired by a cat's gait. The objective was to enhance cat-like robotic mobility by addressing challenges in gait planning and joint coordination. The robot was constructed with 2 degrees of freedom (DoF) for each leg, using lightweight materials such as acrylic, plywood, and aluminum to balance strength and maneuverability. Geometric kinematic equations were applied to model the end-effector positions, and a Fourier series was employed to generate a smooth, periodic trajectory for the foot's end-effector, minimizing jerky movements. The Fourier series fitting achieved high accuracy ($R^2 \approx 0.99$) for the joint angles. The resulting prototype, controlled by an Arduino microcontroller, successfully demonstrated a stable and periodic gait cycle generated through the Fourier series approach, confirming the viability of this kinematic method for straight-line motion.

KEYWORDS: Fourier series; gait cycle; quadruped cat robot; straightforward motion.

1. Introduction

Robotics technology became an important field by enabling tasks that were dangerous or impractical for humans. Among mobile robots, legged robots offered distinct advantages over wheeled counterparts, particularly in navigating uneven terrain. Quadruped robots, inspired by the biomechanics of four-legged animals, provided a balance between stability, control complexity, and adaptability [1–7]. This made them a preferred choice over bipedal and hexapodal robots due to their simpler mechanics and inherent stability.

The design and control of quadruped robots presented significant challenges, including maintaining balance, optimizing gait trajectories, and synchronizing actuator movements in the legs [8–11]. Achieving smooth motion required precise kinematic modeling and dynamic control strategies. While prior studies emphasized the importance of gait planning and joint coordination to replicate natural movement patterns, many prototypes struggled with gait generation and stability during locomotion.

To address these challenges, researchers drew inspiration from biological systems, such as the agility and efficient gait of legged animals, to develop robots with enhanced mobility in real-world environments [12–15]. This bio-inspired robotics approach aimed to simplify locomotion while ensuring adequate mobility. The focus was on developing a straightforward walking motion by modeling the robot's end-effector positions using geometric kinematic equations, allowing trajectory planning that mimicked a quadrupedal gait cycle.

Central pattern generator (CPG)-based controllers for legged robots were often modeled as systems of coupled oscillators, where interactions between oscillators—each corresponding to a joint or leg—produced the rhythmic output that drove the robot's limbs [16–19]. Despite the progress in more complex approaches such as CPGs, simpler kinematic methods like geometric modeling remained relevant for specific applications. These methods relied on solving forward kinematics to determine joint angles for desired leg trajectories. While less adaptive than CPGs, kinematic solutions were computationally efficient and easier to implement, making them suitable for lightweight and cost-effective robot designs.

Gait generation was a critical aspect of legged robot development, determining how the robot coordinated its limbs to achieve locomotion. One effective technique was the use of a Fourier series to generate a smooth, periodic trajectory for the foot's end-effector [20–25]. By transforming discrete angle data into continuous motion, the Fourier series minimized jerky movements. This method used a gait trajectory to determine the end-effector positions over a single gait cycle and then applied Fourier series fitting to create a fluid walking pattern.

This study detailed the development of a quadruped cat robot with 2-DoF legs, constructed from lightweight materials such as acrylic, plywood, and aluminum to balance strength and maneuverability. Geometric kinematic equations were used to model the end-effector positions, and a Fourier series was employed to generate a smooth, cyclical trajectory. The prototype, controlled by an Arduino microcontroller and validated through MATLAB simulations, successfully demonstrated a stable and periodic gait cycle, confirming the viability of this kinematic approach for straightforward motion. The study aimed to contribute to the broader understanding of Fourier-series-based locomotion in quadruped robots. The primary focus was on achieving straightforward walking, where the four-legged robot performed stable and continuous forward motion without incorporating turning maneuvers or terrain adaptations.

2. Materials and Methods

2.1. Material and robot design.

The weight of the quadruped cat robot significantly influenced the selection of actuators required to drive its walking motion. Therefore, a lightweight yet strong structure was essential to support the robot's load and ensure ease of operation. The design also considered the overall form to ensure that each joint conveyed structural integrity. Figure 1(a) illustrates the final design of the quadruped cat robot, developed according to these criteria. The robot's body was constructed using acrylic, which was selected for its superior strength compared to plywood, as it needed to support the entire electrical system. Plywood was chosen for the legs because these components were the primary moving parts; a lightweight yet robust material was necessary to reduce the mechanical load on the servomotors. Aluminum was used for the servo motor mounts since it provided greater strength, durability, and precision compared to PLA-based 3D-printed parts. A standard universal aluminum servo mount was selected to reduce prototype development time. PLA was used only for the foot mounts because using acrylic would have required additional components, resulting in greater overall weight.

(a) (b)

Figure 1. Design and prototype of the cat robot. (a) 3D model of computer-aided design; (b) Resulted prototype.

This material combination resulted in a total robot weight of 1293 g, with final dimensions of 43 cm (length), 20.5 cm (width), and 22 cm (height). The quadruped cat robot was built with 8 degrees of freedom (DOF), with each of the four legs having 2 DOF. The lengths of each limb segment are summarized in Table 1. Most of the robot's body components were laser-cut from plywood, while the leg mounts were fabricated using 3D printing, as shown in Figure 1(b). The robot's movement was powered by eight MG996 standard servo motors, controlled by an Arduino ATmega2560 microcontroller. An LG HE4 18650 Li-ion battery supplied power to the entire system.

Table 1. Link lengths and initial angles.

Link	Link length (mm)	Angle (degree)	Description
L_1	80	30	First link (upper leg segment)
L_2	80	90	Second link (lower leg segment)
L_3	80	90	Third link (passive link connected to L4)
L_4	75	90	Fourth link (passive linkage completing the leg structure)

2.2. Gait generation pattern for forward-motion.

Although the geometric kinematic equations were described briefly, their use followed established practices in legged robot locomotion. Forward kinematics was commonly applied to determine joint configurations for desired leg-tip trajectories [12], providing a simple and efficient alternative to more complex gait-generation methods such as CPG-based approaches [9, 16, 17]. By formulating the leg geometry and simplifying the equations using trigonometric relationships, a complete gait cycle was generated through kinematic modeling. The resulting periodic trajectory was then represented mathematically using curve-fitting techniques such as the Fourier series [22].

This study focused on developing a quadrupedal robot inspired by a cat's structure and movements to achieve a straightforward walking motion. To refine the gait for smoother locomotion, a Fourier series was employed to generate the end-effector trajectory. This method first used a gait trajectory to determine the end-effector positions of the robot's feet over a single gait cycle, followed by applying Fourier-series fitting to the corresponding joint-angle data to produce a smooth and continuous walking pattern. Motion control was subsequently implemented using MATLAB scripts and Simulink blocks that integrated the Fourier-series equations.

2.2.1. Forward kinematics.

Forward kinematics was applied to model the relationship between the robot's joint angles and the resulting positions of its end effectors. In this study, the modeling was performed by deriving geometric equations that defined the robot's leg configuration. These equations were applied to the cat-inspired gait trajectory to determine the corresponding end-effector positions. The gait trajectory was simulated using MATLAB, which generated the required joint angles for each point along the trajectory and enabled detailed analysis of the robot's movement. The geometry of a single robotic leg is shown in Figure 2 as an illustrative example.

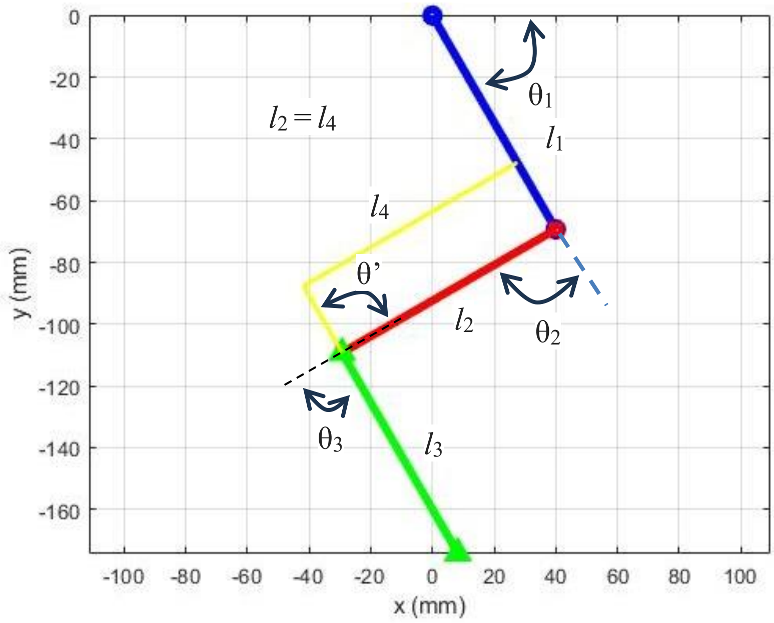

Figure 2. Single Leg Geometry of the cat robot.

The equations used to calculate the end-effector position are presented in Equations (1) and (2). The variables *x* and *y* represent the Cartesian coordinates of the end-effector (the foot tip), measured relative to the hip joint at (0,0). Specifically, *x* denotes the horizontal position of the end-effector, while *y* denotes its vertical position.

$$x = l_1 sin\theta_1 - l_3 \sin(\theta_2 - \theta_1) + l_4 \sin(\theta' - \theta_2 + \theta_1) \quad (1)$$

$$y = -l_1 \cos\theta_1 - l_3 \cos(\theta_2 - \theta_1) - l_4 \cos(\theta' - \theta_2 + \theta_1) \quad (2)$$

The forward kinematics model of the quadruped cat robot was adapted to match the physical structure of the robot's legs. Because one of the links in the cat-like robot is a passive link (link 4), the values of θ_2 and θ_3 were equal. Therefore, based on Equations (1) and (2), the calculation was rewritten according to the robot's leg configuration, resulting in Equations (3) and (4).

$$x = l_1 (sin\theta_1 - \sin(\theta_2 - \theta_1) + l_4 \sin(\theta_1) \quad (3)$$

$$y = -l_1 (\cos\theta_1 + \cos(\theta_2 - \theta_1) - l_4 \cos(\theta_1) \quad (4)$$

By applying the law of sines, Equations (3) and (4) were further simplified to yield Equations (5) and (6).

$$x = l_1 \times 2cos\frac{\theta_2}{2}\sin\left(\frac{2\theta_2-\theta_1}{2}\right) + l_4\sin(\theta_1) \quad (5)$$

$$y = l_1 \times 2sin\frac{\theta_2}{2}\sin\left(\frac{2\theta_2-\theta_1}{2}\right) - l_4\cos(\theta_1) \quad (6)$$

2.2.2. Trajectory generation

Equations (5) and (6) were implemented as a symbolic function in MATLAB, serving as the primary reference for determining the initial position of the robot's leg. Table 1 lists the parameters required for this calculation, including the length of each leg link and the corresponding joint angles. These values were used to compute the joint angles θ_1 and θ_2, which defined the configuration of the leg. Each leg was equipped with two servo motors responsible for actuating θ_1 and θ_2. Based on the kinematic calculation, the end-effector position of the leg was obtained as $x = 8.21$ mm and $y = -174.23$ mm.

To achieve smooth and stable locomotion in the quadruped cat robot, trajectory generation was essential for defining the path of each foot's end-effector throughout a gait cycle. The process began by modeling the initial leg position using forward kinematics to determine the end-effector coordinates based on the parameters summarized in Table 1. Key points along the desired trajectory were then selected to represent the critical phases of the gait, such as lift-off, swing, and touchdown. These points were derived from the robot's kinematic constraints and gait requirements, including stride length and step height. By interpolating between these points, a discrete trajectory was generated and later refined into a continuous motion using a mathematical curve-fitting technique, specifically the Fourier series.

For periodic end-effector trajectory generation, the Fourier series was employed to convert the discrete joint angle data (θ_1 and θ_2) into a smooth and cyclical motion. The Fourier series decomposed the angle profiles into harmonic components, enabling the synthesis of a continuous trajectory that minimized jerky or abrupt movements. In this study, a fifth-order Fourier series was fitted to the angle data using MATLAB's curve-fitting tools, achieving high accuracy ($R^2 \approx 0.99$). A nonlinear least-squares optimization algorithm was applied to determine the Fourier coefficients. The coefficient of determination, R^2, was defined mathematically as shown in Equation (7), where the actual, predicted, and mean values were used for evaluation. The resulting Fourier equations combined sine and cosine terms with empirically derived coefficients, capturing the periodic nature of the gait. This approach ensured fluid, coordinated movement across the gait cycle while reducing the computational load on the microcontroller by compressing the entire trajectory into a compact mathematical form.

$$R^2 = 1 - \frac{\sum_{i=1}^{n}(y_i - \tilde{y}_i)^2}{\sum_{i=1}^{n}(y_i - \bar{y}_i)^2} \quad (7)$$

3. Results and Discussion

3.1. Results.

After modeling the kinematic equations, the next step was to perform trajectory generation, which aimed to determine the leg's end-effector angles throughout a single gait cycle. This process was carried out based on the initial position coordinates previously obtained. The gait cycle pattern was divided into several x- and y-coordinate points, referred to as key points, to define the path that the robot's end-effector would follow. Table 2 presents the coordinate points (key points) used to construct the gait cycle for the robot's leg movement.

Table 2. Position of the gait cycle trajectory.

Key point	x (mm)	y (mm)
1	8	-174
2	-14	-174
3	-5	-150
4	32	-174
5	8	-174

The trajectory generation process for the quadruped cat robot begins with key Point 1, which establishes the robot's initial position. At this stage, the end-effector coordinates (x = 8 mm, y = -174.23 mm) are calculated using forward kinematics, based on the robot's link lengths (L_1–L_4) and initial joint angles ($\theta_1 = 30°$, $\theta_2 = 90°$). The initial position plot is shown in Figure 3. This position serves as the foundation for the gait cycle and is validated through MATLAB modeling (Figure 3). The discrete angles for θ_1 and θ_2 at Key Point 1 provide the baseline data necessary for interpolating the subsequent trajectory points, ensuring a smooth transition to the next phase of end-effector motion.

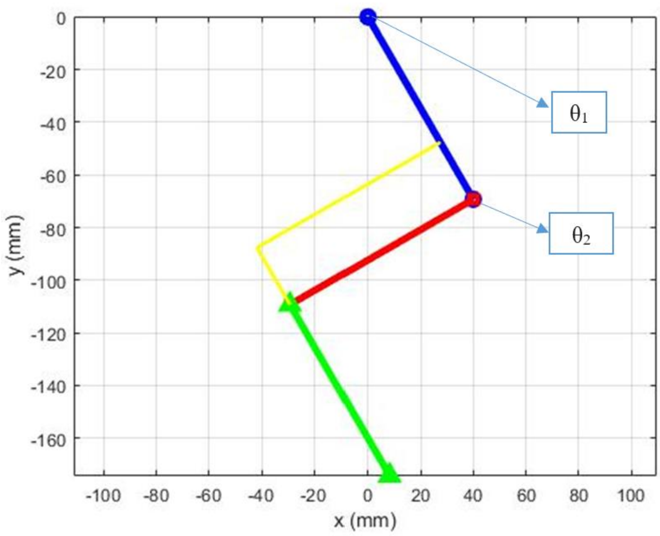

Figure 3. Initial position for the cat robot's leg (key point 1).

From key point 2 to key point 5, the trajectory was generated by interpolating between the predefined coordinates in Table 2 to form a cohesive gait cycle. Key point 2 (x = –14 mm, y = –174.23 mm) represented the backward stride phase, during which θ_1 decreased while θ_2 remained near 90°. Key point 3 (x = –5 mm, y = –150 mm) corresponded to the highest lift during the swing phase, where θ_2 increased to elevate the foot. Key point 4 (x = 32 mm, y = –174.23 mm) indicated the farthest forward reach of the stride, contributing to forward propulsion, while key point 5 returned the leg to its initial position, completing one full cycle. Each transition was computed using MATLAB with a step density of 0.2, ensuring smooth angular changes for both θ_1 and θ_2. The resulting end-effector trajectory for one gait cycle is shown in Figure 4.

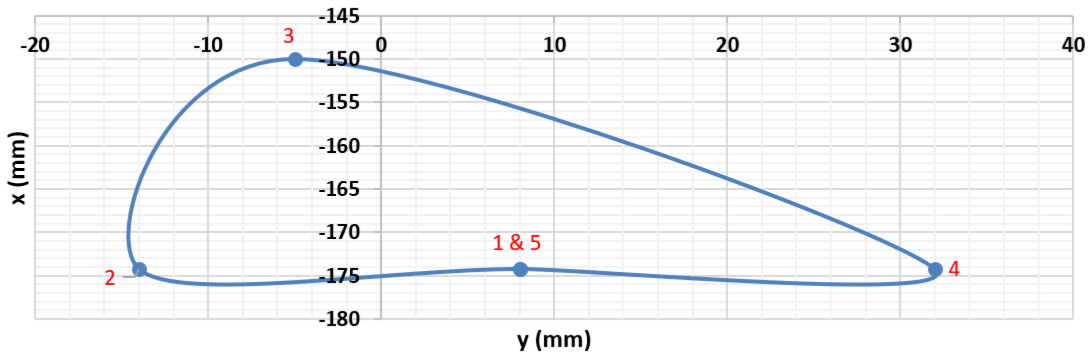

Figure 4. Calculated gait cycle trajectory.

The determination of key points in this study was limited to five points. This limitation was necessary because specifying too many key points would have exceeded the memory capacity of the microcontroller used. The results of the trajectory generation showed that the robot produced a periodic and stable gait cycle. Interpolation between the key points minimized jerky movements, as reflected in the gradual changes in joint angles. Important gait characteristics included sufficient foot clearance during the swing phase (key point 3) and maximum stride length (key point 4), as illustrated in Figure 5 along with the other key points.

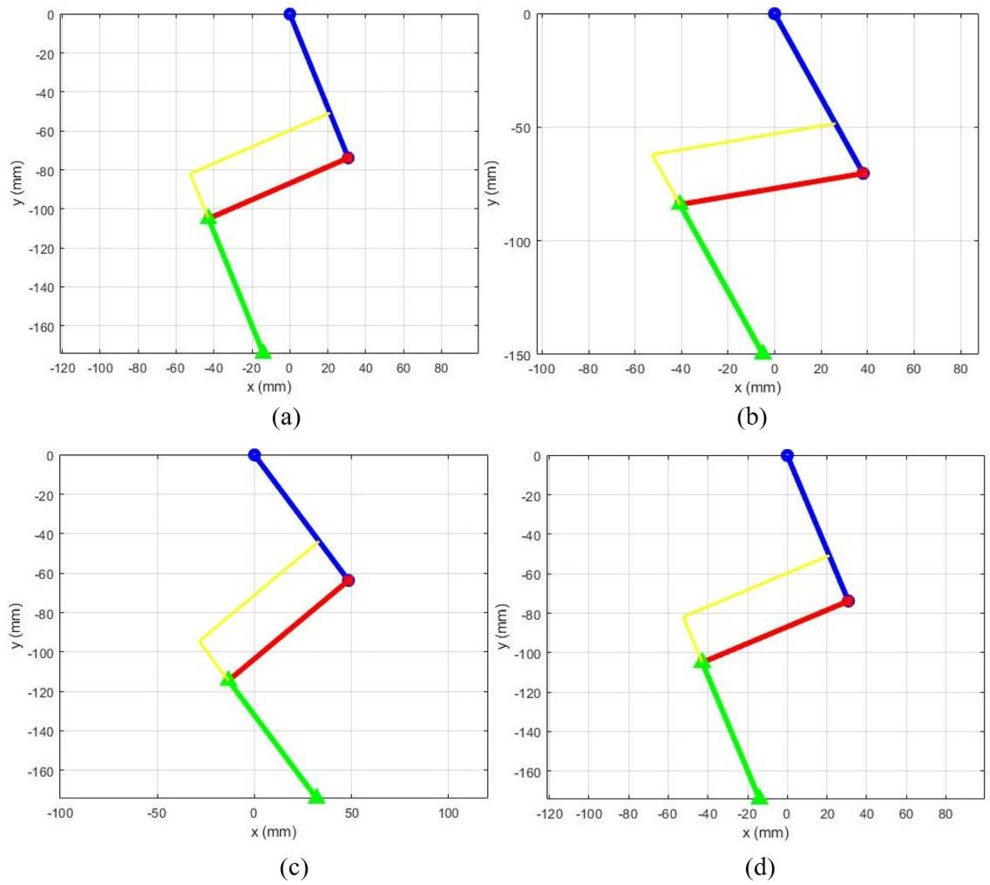

Figure 5. Position for the cat robot's leg. (a) Key point 2. (b) Key point 3. (c) Key point 4. (d) Key point 5.

To achieve smooth and periodic motion of the quadruped cat robot's end effector, a Fourier series curve-fitting approach was applied to the discrete trajectory data. The process began by extracting the joint angle profiles (θ_1 and θ_2) from the gait cycle key points, which were then approximated using a 5th-order Fourier series. For θ_1, the fitting achieved an R^2 value of 0.9991, while θ_2 reached an R^2 of 0.9963, confirming the accuracy of the model. The resulting Fourier equations (Equations 7 and 8) decomposed the angle profiles into harmonic components, enabling efficient real-time control with reduced computational load on the microcontroller.

The joint angles θ_1 and θ_2 , as shown in Equations (8) and (9), are derived from the following Fourier series equations. These equations are used to transform the discrete angle data into continuous, smooth trajectories, which ensures stable and efficient motion control for the robot's gait cycle. Where ω_1 and ω_2 are 5.26 rad/s and 6.28 rad/s respectively.

$$\theta_1(t)=29.78+0.46\cos(\omega_1 t)-6.12\sin(\omega_1 t)-0.31\cos(2\omega_1 t)+0.15\sin(2\omega_1 t)+0.18\cos(3\omega_1 t)+0.56\sin(3\omega_1 t)-0.146\cos(4\omega_1 t)-0.01\sin(4\omega_1 t)+0.06\cos(5\omega_1 t)-0.23\sin(5\omega_1 t) \quad (8)$$

$$\theta_2(t)=94.3-7.60\cos(\omega_2 t)+0.59\sin(\omega_2 t)+4.23\cos(2\omega_2 t)+0.183\sin(2\omega_2 t)-0.68\cos(3\omega_2 t)-0.19\sin(3\omega_2 t)-0.27\cos(4\omega_2 t)-5.89\times10^{-5}\sin(4\omega_2 t)-0.23\cos(5\omega_2 t)+0.05\sin(5\omega_2 t) \quad (9)$$

The quadruped cat robot moved according to the gait cycle trajectory, with angles θ_1 and θ_2 controlled via an embedded MATLAB program. The motion began from the initial position after zero-setting adjustments were made to synchronize the hardware and software. Angle θ_1 reached a maximum of 6.8° at 0.74 seconds and a minimum of –6.8° (counterclockwise) at 0.24 seconds, while θ_2 peaked at 16.7° at 0.5 seconds and dropped to –1.9° at 0.26 seconds, as shown in Figure 6. This motion followed the planned trajectory, with minor deviations attributed to servo motor limitations and insufficient leg rigidity. The results confirmed that the kinematic design for the front right leg operated as intended within a single gait cycle.

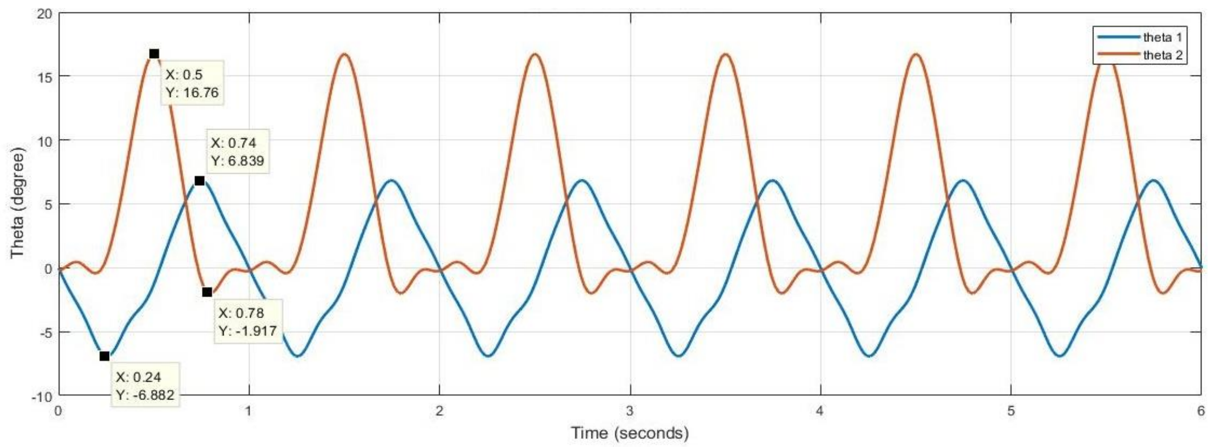

Figure 6. The front right leg movement.

For the front left leg, testing began from key point 3 (rather than the initial position) to establish a movement rhythm opposite to that of the front right leg, causing the left leg to move downward when the right leg lifted. Angle θ_1 reached a maximum of 5.32° at 0.72 seconds and a minimum of –8.39°, while θ_2 peaked at 19.57° at 0.3 seconds and decreased to 0.5° at 0.98 seconds, as shown in Figure 7. The servo motor direction was also adjusted because the initial modeling was based on the right leg. The results demonstrated effective coordination for the trotting pattern, although slight deviations in angles were observed due to servo motor limitations and insufficient leg rigidity.

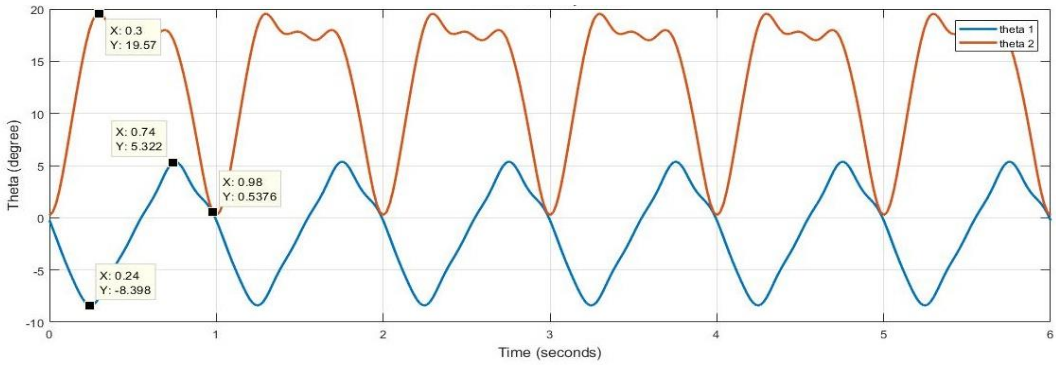

Figure 7. The front left leg movement.

For the rear right leg, the robot moved inversely to the front left leg, starting from key point 3. Angle θ_1 reached a maximum of 8.39° at 0.24 seconds and a minimum of –5.32° at 0.74 seconds. For θ_2, the peak angle was –19.45° at 0.28 seconds, with a minimum of 0° at 0 seconds, as shown in Figure 8. The results demonstrated a coordinated motion pattern, although slight deviations were observed due to servo motor limitations and the leg's limited rigidity.

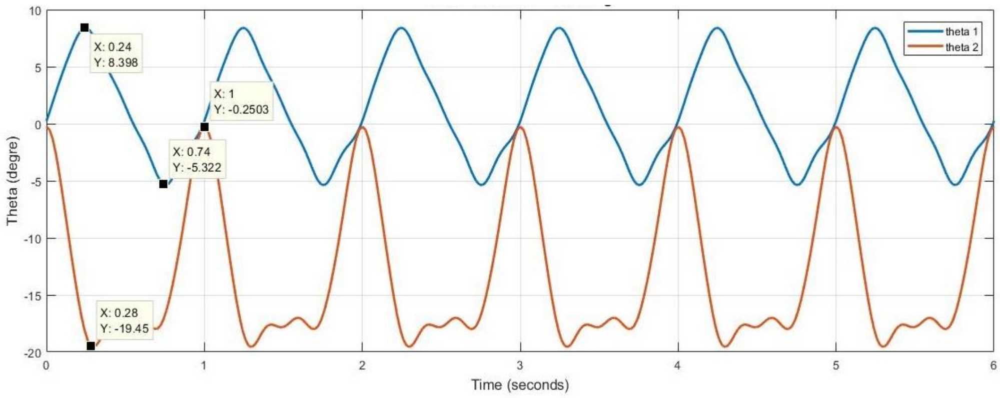

Figure 8. The rear right leg movement.

In the movement of the rear left leg, test results indicate that this leg is the opposite of the front right leg. The maximum angle θ_1 reaches 6.97° at 0.26 seconds, while its minimum is -8.39° at 0.98 seconds. For θ_2, the maximum angle is 2.01° at 0.8 seconds, and the minimum is -16.76° at 0.5 seconds. The movement graph is shown in Figure 9, demonstrating a coordinated motion pattern with other legs to achieve the desired gait trajectory, despite slight deviations due to structural and servo motor limitations.

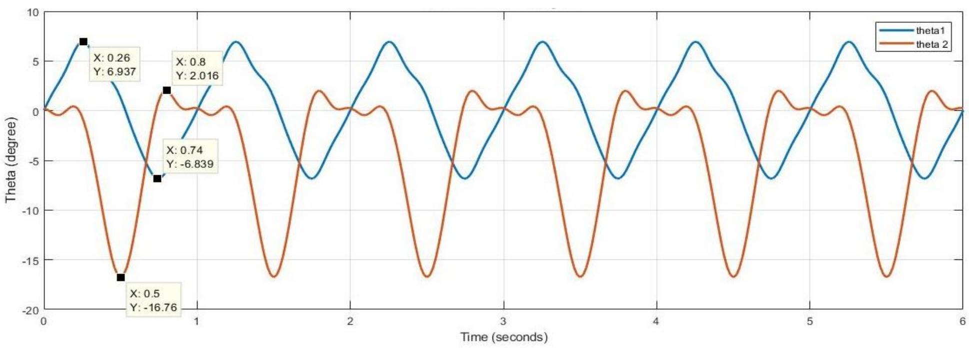

Figure 9. The rear left leg movement.

The results demonstrated that the straightforward motion of the quadruped cat robot, designed using the Fourier series for trajectory generation, was successfully implemented in the prototype, enabling the robot to perform straight movement from left to right, as shown in Figure 10. By applying the Fourier coefficients to model the joint angles θ_1 and θ_2, the robot achieved coordinated leg movements through a trotting gait, with the front right leg moving in sync with the back left leg, and vice versa. Although initial tests revealed challenges such as instability and minor joint deviations caused by structural flexibility and servo motor limitations, adjustments to the components allowed the robot to walk autonomously. The Fourier-based trajectory ensured smooth transitions between key points, validating the kinematic approach for straight motion, while highlighting areas for improvement in dynamic stability in future iterations.

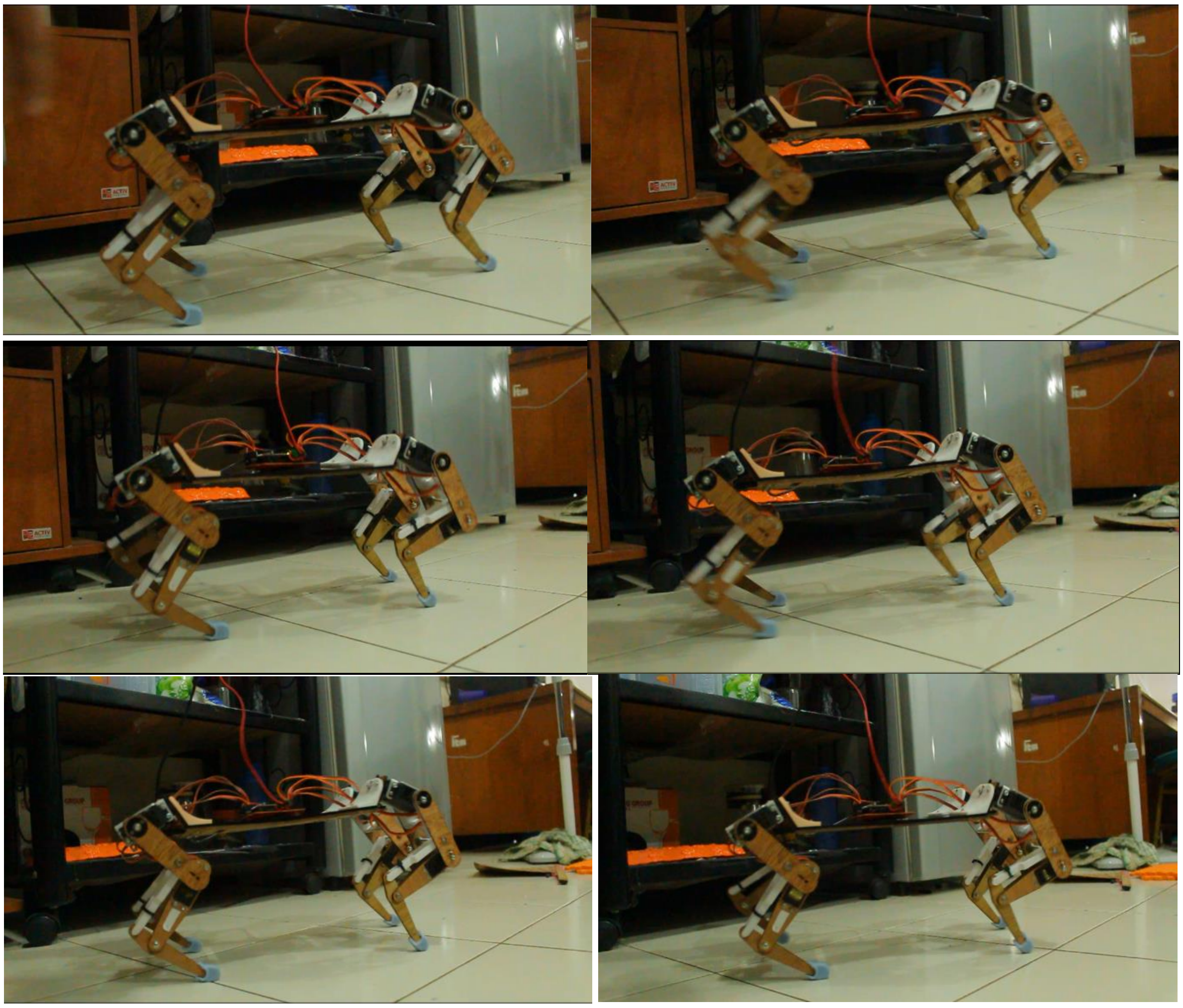

Figure 10. Implemented Fourier series gait generation for straightforward movement on the robot prototype.

3.2. Discussion.

The successful implementation of a Fourier series for trajectory generation in the quadruped cat robot demonstrated the effectiveness of harmonic analysis in simplifying complex gait patterns into smooth, periodic motions. By decomposing the joint angle profiles into Fourier coefficients, the study achieved high accuracy ($R^2 \approx 0.99$ for θ_1 and 0.996 for θ_2), enabling efficient real-time control with minimal computational overhead. The trotting gait, synchronized across diagonally opposed legs (front right with rear left and vice versa), validated the kinematic model.

Despite minor limitations, the robot's ability to perform straight-line motion confirmed the viability of Fourier-based trajectory planning for legged robots. The modular design, combining laser-cut plywood, 3D-printed mounts, and lightweight actuators, proved adaptable for iterative improvements. Future research could enhance stability by integrating feedback control systems, such as IMUs or force sensors, to compensate for real-world disturbances. Additionally, exploring higher-order Fourier terms or alternative optimization algorithms may further refine gait efficiency. This study balanced simplicity and performance, with potential applications in uneven terrain navigation.

The use of a Fourier series aligns with previous works that applied harmonic decomposition to generate smooth and periodic joint trajectories for legged robots, effectively transforming discrete gait data into continuous motion profiles suitable for real-time implementation [22, 25]. The experimental evaluation focused on straightforward walking on flat, controlled surfaces to validate the feasibility of the Fourier-based gait generation method. Future studies will expand experiments across multiple terrains, including quantitative measurements of walking stability, forward speed, and energy consumption.

4. Conclusions

The Fourier series–based trajectory generation enabled the quadruped cat robot to perform a straight-line trotting gait, modeling joint angles θ_1 and θ_2 to ensure smooth transitions and efficient real-time control. Coordinated movement of diagonally opposed legs validated the kinematic model, and the modular design, featuring laser-cut plywood and 3D-printed mounts, allowed adaptability for future improvements. While minor instability and joint deviations occurred due to structural flexibility and servo limitations, the robot successfully achieved autonomous straight-line motion.

Acknowledgments

Funding for this research was partly supported by the Diponegoro University Development and Application Research Grant, contract No. 329-71/UN7.P4.3/PP/2019. The authors would like to thank Mr. Setyo Wisnu Wardana for developing the robot.

Author Contribution

Conceptualization, writing, methodology: M. Munadi; Data acquisition, experiment, funding, writing: Mochammad Ariyanto.

Competing Interest

The authors declare no conflict of interest.

References

[1] Wang, X.; Li, M.; Wang, P.; Guo, W.; Sun, L. (2012). Bio-inspired controller for a robot cheetah with a neural mechanism controlling leg muscles. *Journal of Bionic Engineering*, *9*(3), 282–293. http://doi.org/10.1016/S1672-6529(11)60120-0.

[2] Majithia, A.; Shah, D.; Dave, J.; Kumar, A.; Rathee, S.; Dogra, N.; Vishwanatha, H.M.; Chiniwar, D.S.; Hiremath, S. (2024). Design, motions, capabilities, and applications of quadruped robots: a

comprehensive review. *Frontiers in Mechanical Engineering*, *10*, 1448681. http://doi.org/10.3389/fmech.2024.1448681.

[3] Abdulwahab, A.H.; Mazlan, A.Z.A.; Hawary, A.F.; Hadi, N.H. (2023). Quadruped robots mechanism, structural design, energy, gait, stability, and actuators: a review study. *International Journal of Mechanical Engineering & Robotic Research*, *12*(6), 385–395. http://doi.org/10.18178/ijmerr.12.6.385-395.

[4] Li, Q.; Cicirelli, F.; Vinci, A.; Guerrieri, A.; Qi, W.; Fortino, G. (2025). Quadruped robots: bridging mechanical design, control, and applications. *Robotics*, *14*(5), 57. http://doi.org/10.3390/robotics14050057.

[5] Chatzakos, P.; Papadopoulos, E. (2009). Self-stabilising quadrupedal running by mechanical design. *Applied Bionics and Biomechanics*, *6*(1), 748719. http://doi.org/10.1080/11762320902863908.

[6] Stella, F.; Achkar, M.M.; Della Santina, C.; Hughes, J. (2025). Synergy-based robotic quadruped leveraging passivity for natural intelligence and behavioural diversity. *Nature Machine Intelligence*, *7*(3), 386–399. http://doi.org/10.1038/s42256-025-00988-x.

[7] Holmes, P.; Full, R.J.; Koditschek, D.; Guckenheimer, J. (2006). The dynamics of legged locomotion: models, analyses, and challenges. *SIAM Review*, *48*(2), 207–304. http://doi.org/10.1137/S0036144504445133.

[8] Zhang, Y.; Liu, W.; Tan, N. (2024). Motion control of legged robots based on gradient central pattern generators. *Robotica*, *42*(9), 3102–3131. http://doi.org/10.1017/S0263574724001309.

[9] Liu, C.; Chen, Q.; Wang, D. (2011). CPG-inspired workspace trajectory generation and adaptive locomotion control for quadruped robots. *IEEE Transactions on Systems, Man, and Cybernetics, Part B (Cybernetics)*, *41*(3), 867–880. http://doi.org/10.1109/TSMCB.2010.2097589.

[10] Hernández-Flores, E. A.; Hernández-Rodríguez, Y. M.; Munguía-Fuentes, R.; Bayareh-Mancilla, R.; Cigarroa-Mayorga, O. E. (2024). *Acinonyx jubatus*-inspired quadruped robotics: integrating neural oscillators for enhanced locomotion control. *Biomimetics*, *9*(6), 318. http://doi.org/10.3390/biomimetics9060318.

[11] Fan, Y.; Pei, Z.; Wang, C.; Li, M.; Tang, Z.; Liu, Q. (2024). A review of quadruped robots: structure, control, and autonomous motion. *Advanced Intelligent Systems*, *6*(6), 2300783. http://doi.org/10.1002/aisy.202300783.

[12] Ariyanto, M.; Munadi, M.; Setiawan, J.D.; Wardana, S.W. (2019). Design and kinematic analysis of quadrupedal cat-like robot. 2019 International Seminar on Research of Information Technology and Intelligent Systems (ISRITI), pp. 398–402. http://doi.org/10.1109/ISRITI48646.2019.9034577.

[13] Wieber, P.-B.; Tedrake, R.; Kuindersma, S. (2016). Modeling and control of legged robots. In Springer Handbook of Robotics. Siciliano, B., Khatib, O., Eds.; Cham: Springer International Publishing, pp. 1203–1234. https://doi.org/10.1007/978-3-319-32552-1_48.

[14] Zhao, Y.; Wang, J.; Cao, G.; Yuan, Y.; Yao, X.; Qi, L. (2023). Intelligent control of multilegged robot smooth motion: a review. *IEEE Access*, *11*, 86645–86685. http://doi.org/10.1109/ACCESS.2023.3304992.

[15] Azeez, S.A.; Mandava, R.K.; Naik, N.S. (2025). A novel review on quadruped robots design variants, gait modulation, and motion planning schemes. *Journal of Field Robotics, 42,* 3615–3693. http://doi.org/10.1002/rob.22575.

[16] Munadi, M.; Ariyanto, M.; Pambudi, K.A.; Setiawan, J.D. (2019). Development of 18 DOF salamander robot using CPG-based locomotion for straight forward walk. *International Review of Mechanical Engineering*, *13* (1), 70–77. http://doi.org/10.15866/ireme.v13i1.16464.

[17] Ijspeert, A.J. (2008). Central pattern generators for locomotion control in animals and robots: a review. *Neural Networks*, *2* (4), 642–653. http://doi.org/10.1016/j.neunet.2008.03.014.

[18] Liu, G.L.; Habib, M.K.; Watanabe, K.; Izumi, K. (2008). Central pattern generators based on Matsuoka oscillators for the locomotion of biped robots. *Artificial Life and Robotics*, *12*(1), 264–269. http://doi.org/10.1007/s10015-007-0479-z.

[19] Yu, H.; Guo, W.; Deng, J.; Li, M.; Cai, H. (2013). A CPG-based locomotion control architecture for a hexapod robot. IEEE/RSJ International Conference on Intelligent Robots and Systems, November 2013, pp. 5615–5621. http://doi.org/10.1109/IROS.2013.6697170.

[20] Zhang, S.; Zhang, Y.; Luan, M.; Peng, A.; Ye, J.; Chen, G. (2025). Generation & clinical validation of individualized gait trajectory for stroke patients based on lower limb exoskeleton robot. *IEEE Transactions on Automation Science and Engineering*, *22*, 6463–6474. http://doi.org/10.1109/TASE.2024.3445886.

[21] Anh, H.P.H.; Huan, T.T. (2020). Optimal walking gait generator for biped robot using modified Jaya optimization technique. *International Journal of Computational Intelligence Systems*, *13*(1), 382–399. http://doi.org/10.2991/ijcis.d.200323.001.

[22] Kim, J.-Y.; Kim, Y.-S. (2010). Human-like gait generation for biped android robot using motion capture and ZMP measurement system. *International Journal of Humanoid Robotics*, *7*(4), 511–534. http://doi.org/10.1142/S0219843610002155.

[23] Zamiri, A.; Farzad, A.; Saboori, E.; Rouhani, M.; Naghibzadeh, M.; Fard, A. M. (2008). An evolutionary gait generator with online parameter adjustment for humanoid robots. IEEE/ACS International Conference on Computer Systems and Applications, March 2008, pp. 9–14. http://doi.org/10.1109/AICCSA.2008.4493510.

[24] Park, I.-W.; Kim, J.-Y. (2010). Fourier series-based walking pattern generation for a biped humanoid robot. 10th IEEE-RAS International Conference on Humanoid Robots, December 2010, pp. 461–467. http://doi.org/10.1109/ICHR.2010.5686303.

[25] Shafii, N.; Khorsandian, A.; Abdolmaleki, A.; Jozi, B. (2009). An optimized gait generator based on Fourier series towards fast and robust biped locomotion involving arms swing. IEEE International Conference on Automation and Logistics, August 2009, pp. 2018–2023. http://doi.org/10.1109/ICAL.2009.5262600.